International Journal of Industry and Sustainable Development (IJISD), Volume 5, Issue 1, 2024

Print ISSN 2682-3993
Online ISSN 2682-4000

Effects of FMWCNT inclusions on PVDF/FMWCNT membranes structure and characteristics

R.M.Zarraa[1,2] , Shaaban Nosier[3], A.A. Zatout[3], MH Abdel-Aziz[3,4] , Mohammed S.Al-Geundi[2]

[1]Petrochemical Engineering Department, Faculty of Engineering, Pharos University in Alexandria, Alexandria, Egypt.
[2] Chemical Engineering Department, Faculty of Engineering, Minia University, Minia, Egypt.
[3]Chemical Engineering Department, Faculty of Engineering, Alexandria University, Alexandria, Egypt.
[4]King Abdulaziz University, Chemical and Materials Engineering Department, Rabigh, Saudi Arabia.
Radwa.zarraa@pua.edu.eg , nosier2017@gmail.com , ahmed.zaatoot@alexu.edu.eg , mhmossa@kau.edu.sa , m.zaghlul@mu.edu.eg

Abstract: Commercial polyvinylidene difluoride (PVDF) membrane and another membrane which was composed of PVDF and FMWCNTs used to remove organic compounds from a water using the vacuum membrane distillation (VMD) method. SEM analysis, FTIR, and contact angle to examine the pore size and porosity and the hydrophobicity nature of the membrane to establish the permeate side’s quality and quantity, the properties of PVDF/FMWCNTs nanocomposites (NCs), which were created by phase inversion, and the crystal structure of poly(vinylidene fluoride) (PVDF) were examined in relation to the effects of multiwall carbon nanotube (MWCNT) inclusions. Our results suggest that the effects of FMWCNT inclusions on the PVDF crystallization process are highly dependent on the exact melt treatment and subsequent cooling procedure. The addition of FMWCNTs causes the membrane's porosity and mass transport-available pores to rise. It also decreases hydrophobicity, as seen by the sudden decline in the contact angle. The fabricated membranes conducted in VMD cell to evaluate the total permeate reflux of ethanol separation from ethanol water mixture.

***Keywords*:** Phase inversion, FTIR,Contact angle ,Hydrophobic,Sem

1. INTRODUCTION

Commercially, for membrane distillation applications, numerous membranes made of polymers are used. Solvent casting is used to create these polymeric membranes, which use a process called nonsolvent induced phase separation (NIPS). Commercial microporous membranes formerly been produced using a number of various solvents. It is soluble in dimethylsulfonic acid, dimethylacetamide, dimethylformamide and insoluble in ketones and esters. It has high mechanical strength, wear and weather resistance, resistance to ultraviolet and ionizing radiation, the action of mineral acids, with the exception of fuming sulfuric, alkalis, halogens and hydrocarbons. [1]**.** These solvents fall under the hazardous category and are toxic to the environment [2,3]. Therefore, nonhazardous solvent use in industry is recommended. An eco-friendly solvent classified as a safe, environmentally friendly solvent is dimethyl sulfoxide (DMSO) [4,5].

Membrane distillation (MD) has a lot of drawbacks. One of them is the requirement for membranes with particular properties to guarantee successful operation and long-lasting performance. The membrane wetting phenomenon is one of the main disadvantages of MD, which is mostly caused by the working liquids wetting the membrane pores [6].

Furthermore, membranes were changed by being blended with different polymers [7,8], compatibility between polymers and additives [9], the addition of inorganic fillers and surface modifications [10–13], to enhance their properties and performance. The kind of a solvent and polymeric material, the solution for dope temperature, composition of the coagulation agent, temperature of the bath of coagulation, timing of evaporation, and dry circumstances are only a few of the factors that affect membrane properties. According to specific separation objectives, modifications are done. When separating ethanol from water using MD, for instance, membrane hydrophobicity is one of the most desired

Print ISSN 2682-3993
Online ISSN 2682-4000

parameters. Due to their reduced water molecule interaction with the membrane surface, hydrophobic membranes improve the performance of MD [14].

In regions where solar irradiance and water scarcity are closely associated, using solar thermal energy for membrane distillation desalination provides a safe and environmentally friendly solution [15]. To explore the energy-saving through heat recovery, an air gap membrane distillation (AGMD) unit underwent experimental research.. The water desalination plant made use of the module for spiral air gap membrane [16]. The lack of freshwater worldwide and the rising cost of fossil fuels have spurred the development of new and energy-efficient desalination methods [17]. Governments are burdened by the water constraint as a result of the rapid population growth and expansion of industry. Innovative water delivery systems with minimal production costs must be developed immediately [18], novel techniques like forward osmosis (FO) and membrane distillation (MD) demonstrated extraordinary operational stability in the presence of heavy oil and salt concentrations [19].

Poly(vinylidene fluoride) (PVDF) is an engineering thermoplastic fluoropolymer that finds extensive use in a multitude of sectors, including lithium batteries, sensors and transducers, insulation, and biomedical applications. Because of its easy processability, mechanical strength, low weight, low thermal conductivity, strong chemical corrosion resistance, and heat resistance, it is used in the variety of applications listed above [20–22]

Therefore, because to its hydrophobic properties and simple solubilization in a variety of organic solvents, polyvinylidene fluoride (PVDF) is the polymer that is most typically employed to create commercial membranes. greater hydrophobicity is implied by a greater CA.

For the purpose of purifying water, different nanomaterials such Zeolites, dendrimers, carbon nanomaterials, and metal/metal oxide nanoparticles have seen tremendous revolutions the past few years. Due to their distinctive characteristics, including as their huge surface area, high length to diameter ratio, and great mechanical strength, FMWCNTs have been shown to be efficient as one-dimensional additives in the production of membranes [23]. FMWCNTs exceptional capacity for mass transfer through their inner channels makes them potentially useful as membrane nanofillers. The water flux produced by the membrane made entirely of FMWCNTs was greater than the water flux measured using PVDF membrane [24–27]. Additionally, by using FMWCNTs in the membrane matrix, both the antifouling property and mechanical strength have been enhanced [28,29].

Applying contact angle, Fourier transform infrared (FTIR), and scanning electron microscopy, porosity, and pH range, the purpose of this work is to create and characterize flat sheet PVDF & PVDF FMWCNTs polymeric membranes as well as study the phase inversion-prepared PVDF and PVDF/FMWCNTs nanocomposites' (NCs) shape, structure, and mechanical characteristics.

2. MATERIALS AND METHODS

I. Membrane Preparation

In order to remove unbounded moisture before membrane fabrication, PVDF polymers were dried in a vacuum oven. Molecular weight of PVDF is above 100,000 g/mol, melting point is of 171–180 °C, the crystallization temperature is of 141–151 °C, and a glass transition temperature is of −40 °C. Phase inversion was employed to create flat sheet membranes, with distilled water serving as the coagulation medium. Phase inversion, which involved the solvent-nonsolvent de mixing process and solvent evaporation, converted the solution of dope into a solid form. The basic polymer (PVDF) was used to manufacture the dope solutions, Then subsequently agitated at 150 rpm with a stirring magnet for 6 hours at 60°C and 6 hours at 70°C to produce an evenly distributed polymeric solution for dope. After being kept for 24 hours to allow for degassing, the homogeneous polymeric solution was cast onto a plate of glass with an unwoven material providing support for the membrane To get rid of the solvents, the plate of glass was immersed instantly in a bath of coagulation for twenty-four hours, using distilled water as the non-solvent. The manufactured membrane was dried after complete mixing for 48 hours at ambient temperature, then dried again at 70°C vacuum oven to eliminate any leftover solvent and non-solvent that had become confined inside the matrix of membranes[30,31].

Print ISSN 2682-3993
Online ISSN 2682-4000

II. Preparation of FMWCNTs /PVDF membrane

In general, by increasing FMWCNTs, as a hydrophilic element, some walls membrane between the internal channels of the membrane are lost and large interconnected pores are formed due to increased placement velocity of solvent and nonsolvent during the phase inversion process. These interconnected pores may increase the porosity and water flux of the related mem-branes. FMWCNTs with carboxylic acid and hydroxyl groups, respectively with diameters of 10–50 nm and length of 1–30 µm (from Nanjing XF Nanomaterial Science and Technology Co) FWCNTs were dispersed in NMP using ultrasonication for 12 hours as part of the preparation phase for the FMWCNTs/PVDF solution to prevent agglomeration. In the meantime, NMP (30 wt%) was used to dissolve PVDF pellets in an oven at 70 °C for two hours [32]. The final solution was then created by sonicating the PVDF/ NMP solution for 12 hours with the MWCNT suspension. FMWCNTs made up 0.2% of the FMWCNTs/PVDF mixture. As depicted in figure 1 [33–35].

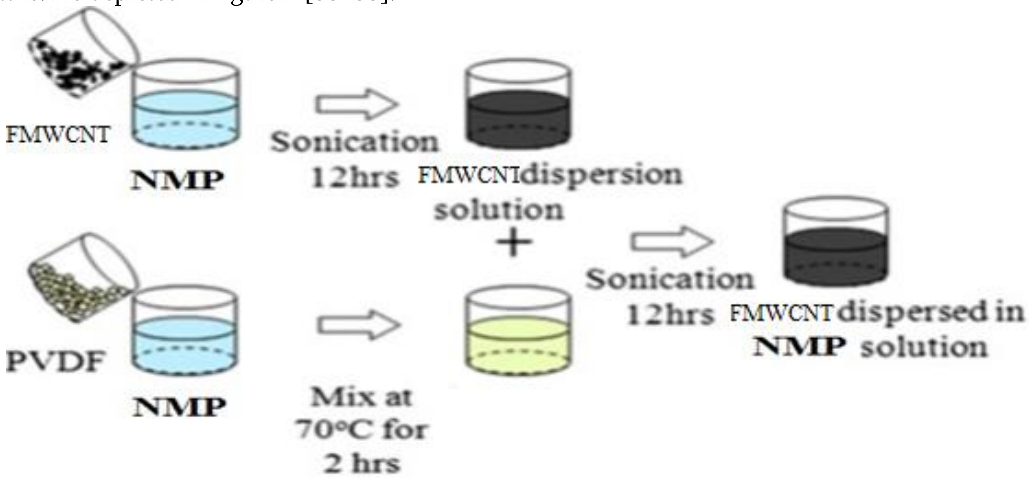

Figure 1 Preparation of membrane of PVDF with FMWCNTs

III. Vacuum Membrane Distillation Cell

A vacuum membrane distillation cell (VMDC) utilized in the current study to evaluate the separation of alcohol from water using the tow fabricated membranes by study the rate of flux. shown in Figure 2, the membrane cell made of two separate compartments made of acrylic polymeric material to prevent corrosion and to avoid the dissolving by the ethanol solution. The outer area of the cell is 54 m2 and the fabricated membrane of 16 m2 was inserted in the middle of cell between the two polymeric compartments. The polymeric membrane separates the cell into two chambers. The down part of cell contains two parts, one for entering the feed solution and the other part for which Leaving the retentate which recycled again to the feeding tank. The distance between the two parts was about 2cm. A vacuum using a vacuum pump was applied to other party cell (Upper party or permeate part) The permeate was obtained by condensing the fluxed vapor leaving the upper part of cell using Cold water that circulated through the condenser. The Condensed vapor (Permeate) leaving the condenser was collected in permeate tank. The mixture of ethanol and water used was 2% wt concentration, the temperature of feed solution was 50°C and the volumetric flow rate of feed solution used in the present work 0.143 L/min. The total permeates flux was determined by the following equation(1) [36,37].

$$J_{tot} = \frac{w_p}{A \times t} \qquad (1)$$

Print ISSN 2682-3993
Online ISSN 2682-4000

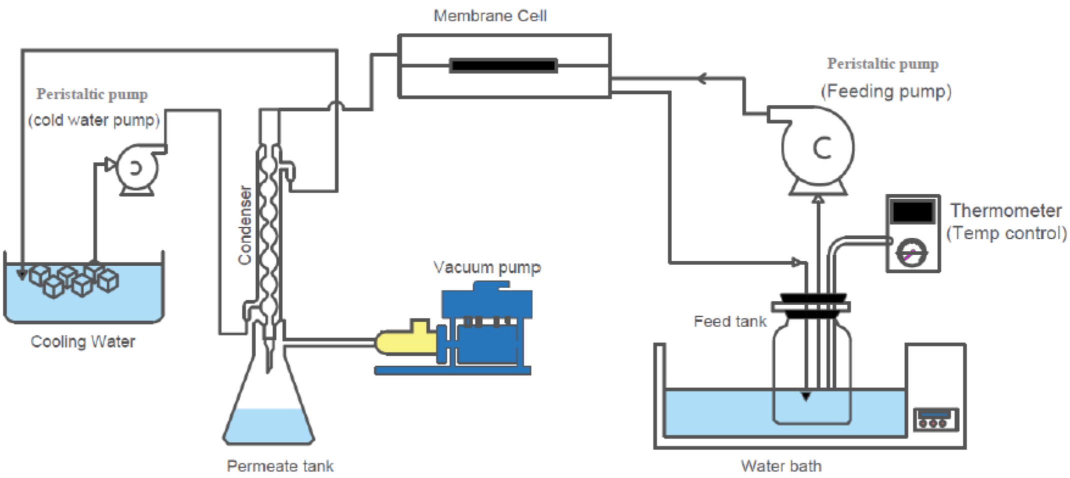

Fig 2. Schematic Representation of the Laboratory-Scale Vacuum Membrane Distillation Apparatus

3. MEMBRANE CHARACTERIZATION

I. Scanning Electron Microscopy

Scanning electron microscopy (SEM) was utilized to exhibit the morphology of the generated membranes. To increase electrical conductivity, gold was applied to the membrane sample surfaces. A SEM TESCAN (3 XMU, MIRA) was used to scan the top surface of membranes to reveal their holes [38].

II. Fourier Transform Infrared Spectroscopy

One of the best techniques for sample characterization is Fourier transform infrared (FTIR) spectroscopy, it could be applied to determine the functional groups and potential molecular interactions between chemical compounds. FTIR can be used for both quantitative and qualitative analysis, and it can be employed with a variety of materials and circumstances. The instrument used to determine a sample's absorbance spectrum is a spectrophotometer. The FTIR spectrophotometer (Bruker, Alpha) provides the IR spectrum significantly more quickly than the conventional spectrophotometer[39].

III. Contact Angle

The hydrophilicity and the contact angle determine the membrane surface's moisture absorption capacity. A tiny video microscope was used to measure the contact angle (CVM). The average drop volume was 10l, and the contact time was 10 s. Each figure was the average of ten measures that are repeated. The testing procedure is based on Standard procedures for corona-treated polymer films, ASTM D5946-96 employing measurements of the water contact angle and the standard testing method for paper's surface wetness is ASTM D724-99 [40].

IV. Membrane Porosity

The density as shown in the following equation can be employed in the computation of membrane porosity. After being submerged in isopropanol for six hours, the membrane was dried with paper towels. Equation (2) was used to determine the porosity by measuring the weight of the wiped-and-dried membrane.

$$= \frac{m_b/\rho_b}{m_b/\rho_b + m_p/\rho_p} * 100\% \qquad (2)$$

ε= the membrane's porosity m_b= membrane mass(g)

Print ISSN 2682-3993
Online ISSN 2682-4000

m_p= isopropanol absorbed mass (g) ρ_b= membrane density (g/cm^3)

ρ_b= isopropanol density (g/cm^3) [41].

V. Pore Size

With the aid of the The University of Wisconsin, Madison, WI, USA's ImageJ software (LOCI), the average pore size of PVDF membrane was calculated [42].

VI. Tensile Strength Measurements

The tensile tests of the fabricated membranes, PVDF and FMWCNTs/PVDF , were carried out using a Universal Mechanical and Tribological Tester UMT-2M (Bruker) at room temperature. The samples were clamped at both ends and pulled at constant elongation velocity of 0.1 mm/sec. Ultimate Tensile strength was obtained [43].

Table 1 summary of all devices model used for analysis of the membranes

Analysis Test	Device	purpose
Scanning Electron Microscopy	A SEM TESCAN (3 XMU, MIRA	Exhibit the morphology of the generated membranes
Fourier Transform Infrared Spectroscopy	FTIR spectrophotometer (Bruker, Alpha	Determine the functional groups
Measurements of the water contact angle	ASTM D5946-96	• Hydrophilicity • Contact angle • Membrane surface's moisture
***A*verage pore size**	University of Wisconsin, Madison, WI, USA's ImageJ software (LOCI)	Determine Pore Size
Tensile Strength Measurements	Universal Mechanical and Tribological Tester UMT-2M (Bruker)	Ultimate Tensile strength was obtained

4. RESULTS AND DISCUSSIONS

I. Scanning Electron Microscopy

The SEM imaging of the PVDF membrane and the investigation of PVDF/CNTs are shown in Figure 3(a,b). The porosity of the manufactured two membranes was shown by the SEM imaging, which was carried out at an accelerating voltage of 15 kV. As we can see, the PVDF has entirely covered the FMWCNTs, leaving FMWCNT remnants around the top and bottom borders. Due to the addition of CNTs, the surface is smooth ("skin type"), homogeneous, and has a greater number of pores, which implies a declining hydrophobicity.

Print ISSN 2682-3993
Online ISSN 2682-4000

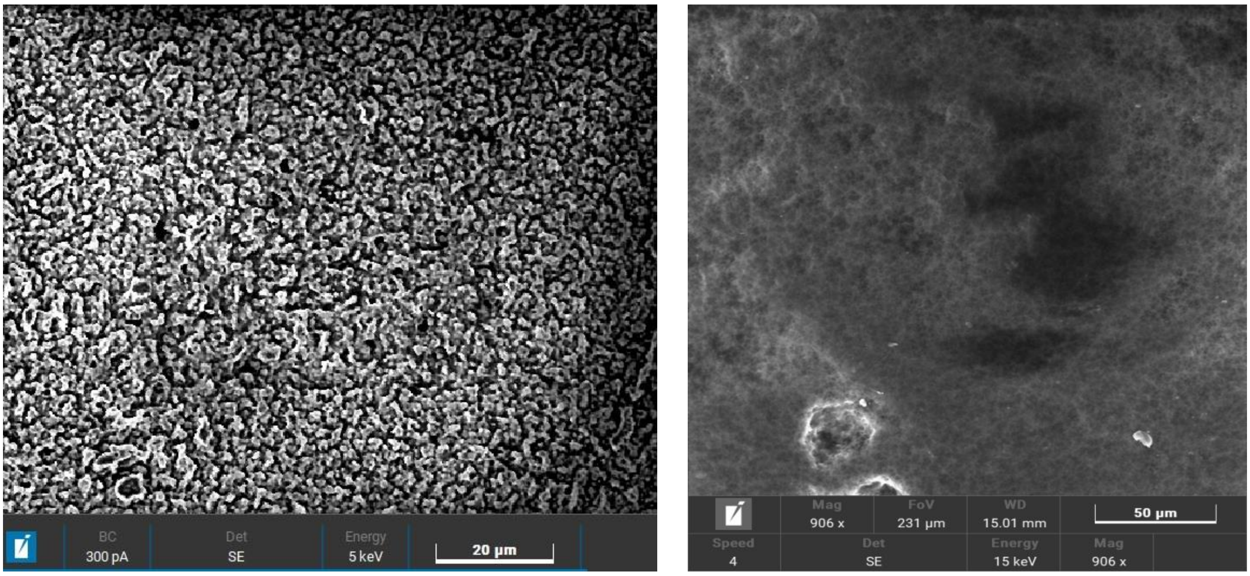

Figure 3 (a,b) SEM of PVDF membrane and PVDF/CNTs membrane

II. Porosity and contact angle

By using the water contact angle test, the hydrophobicity of the PVDF and MWCNT/ PVDF membranes was evaluated. In this test, the contact angle between the membrane sample and the deionized water was measured and contrasted with the membrane sample's contact angle. and the methylene blue. The contact angle was tested twice with various drop phases; the results show that the contact angles for PVDF and MWCNT membranes are (110°) and (92°), respectively. To confirm the reproducibility of the results, the membrane porosity test was conducted three times. By replacing in equation (2), it was discovered that the membrane porosity for PVDF and MWCNT PVDF membranes, respectively, is equal to 45.6% and 71.2%. The essential properties of membranes are outlined in Table 2 [44,45].

Table 2 Main Characteristics of PVDF membrane and PVDF/FMWCNTs membrane

Membrane	**Porosity**	**Contact angle**	**Pore size**	**Tensile strength**	**PH range**
PVDF	45.6%	110°	0.22µm	4.5MPa	2-10
FMWCNT PVDF	71.2%	92°	0.45 µm	42.4MPa	3-9

III. Fourier Transform Infrared Spectrometer (FTIR)

Fourier Transform Infrared Spectrometer (FTIR) displays the phases and active bonds in the membrane structure. As demonstrated in Figure 4 a,b. Peaks at 3305,2948 cm^{-1} reveals the carboxylic acid O–H stretch appears. The peaks at 1406 and 870 cm^{-1} show $CH2$ deformation and rocking vibrations, respectively, while that at 1095 cm^{-1} is assigned to $C{-}F$ wagging vibration. Moreover, distinctive bands at 1043, 1035, and 791 cm^{-1} belongs to $CF2$ bending, deforming, and stretching vibrations. The presence of the α-phase is another characteristic of a $PVDF$ membrane. at 719 cm^{-1} and existence of Y-phase at 1241 and 433 cm^{-1}.

Following the addition of MWCNTs to PVDF, the stretching modes C-F (830-900 cm^{-1}) and C-N (1200–1500 cm^{-1}) with corresponding vibrations in the signature of PVDF and FMWCNTs are apparent in the FTIR [46,47]. The signals of C-C, C-O, and C-H are either extremely faint or invisible since FMWCNTs were very low in concentration compared to PVDF throughout the method of

Print ISSN 2682-3993
Online ISSN 2682-4000

coating. The likelihoods might result from the substantial PVDF coating and low MWCNT concentration [42,48,49].
Mass movement through the membrane might be aided by a higher membrane porosity, larger mean pore size, and a thinner layer of membrane. Although the flux through the membrane could not be raised as feed velocity increased, the mass transfer resistance across the membrane might predominate at a higher feed flow rate. The total permeate flux increased significantly when FMWCNTs were added to the PVDF membrane because the membrane's hydrophobicity decreased, as evidenced by the membrane's decreasing contact angle when FMWCNTs were added compared to when they weren't [42,46,49].

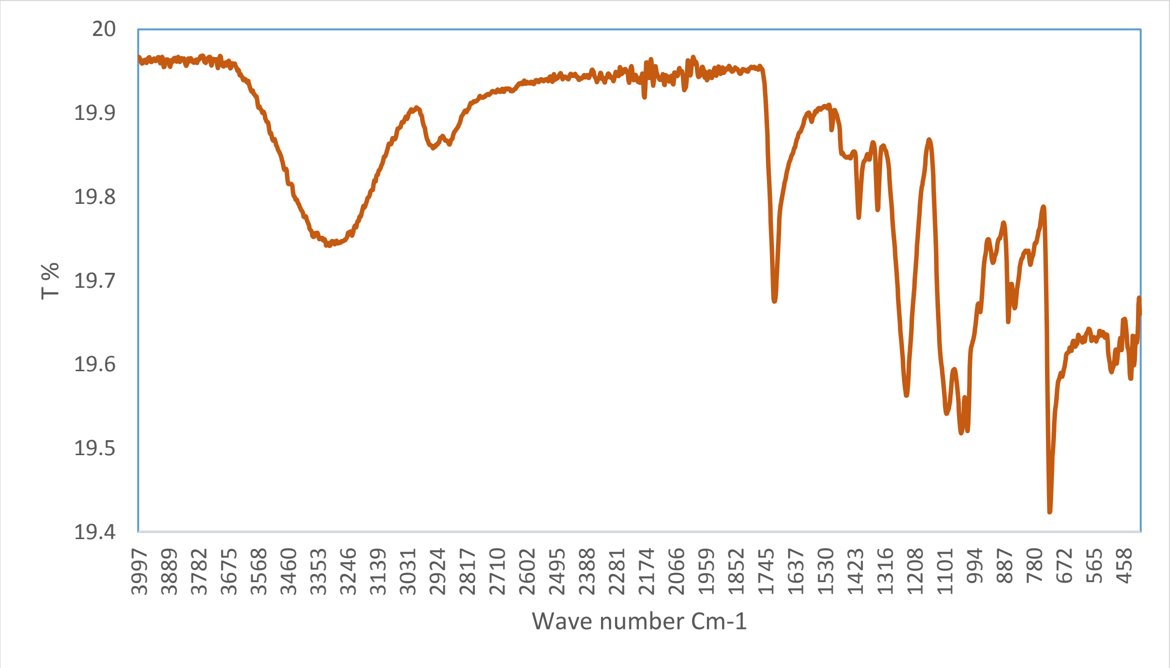

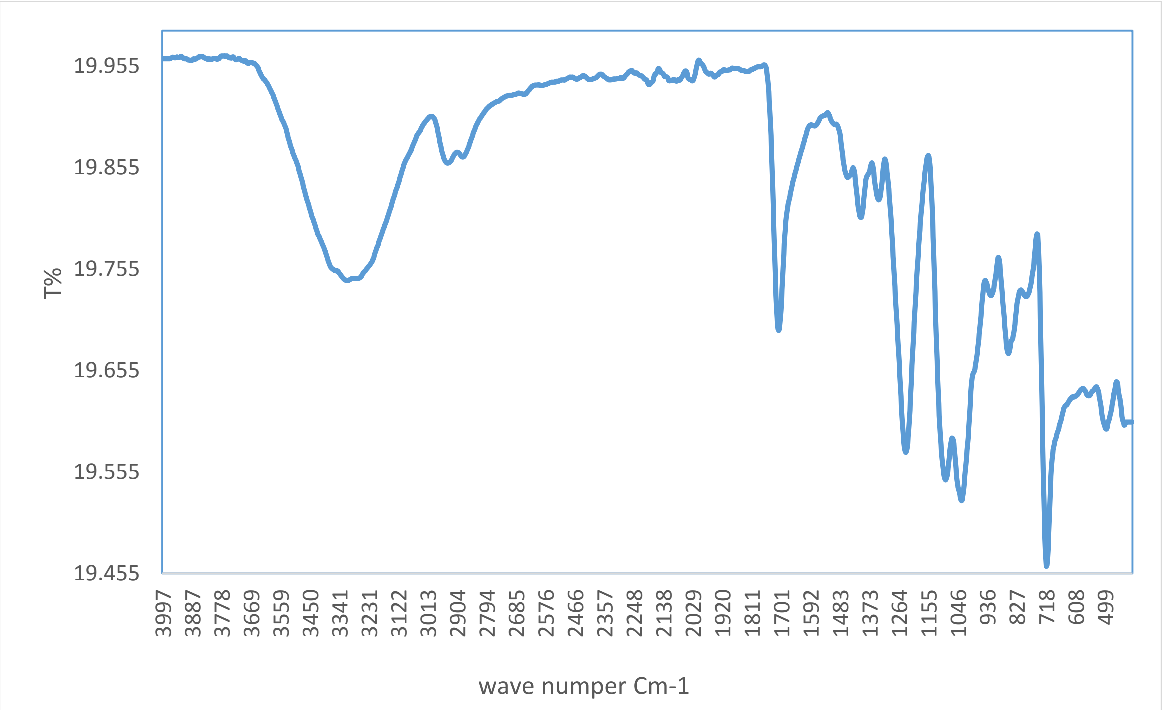

Figure 4a,b PVDF membrane and PVDF/MWCNTs FTIR

Print ISSN 2682-3993
Online ISSN 2682-4000

IV. Total permeate flux

It can be seen that; the total permeate flux was increased using PVDF/FMWCNTs membrane compared with pure PVDF membrane due to the hydrophobicity of membrane renders it highly selective to the ethanol than water. as showed in Table 3.

Table 3 Total permeate flux of ethanol separation from ethanol water mixture

Membrane	Feed flow Rate	Feed Temperature	Ethanol Concentration	Total permeate flux (Kg / m^2.hr)	Percent Increase %
PVDF	0.143 L/min	50°C	2% wt	35.8375	
PVDF/FMWCNTs	0.143 L/min	50°C	2% wt	47.175	31.63%

5. CONCLUSIONS

In this research, we looked at how melt-mixed PVDF/FMWCNTs nanocomposites (NCs) with FMWCNTs inclusions changed PVDF's crystalline structure and dielectric characteristics. Our findings imply that the precise melt treatment and subsequent cooling process have a significant impact on the impacts of FMWCNT inclusions on the PVDF crystallization process. Adding FMWCNTs leads to an increase porosity of the membrane and the pores available for mass transport and also decrease hydrophobicity which was demonstrated by the abrupt decline in the contact angle. A vacuum membrane distillation cell (VMDC) utilized in the current study to evaluate the separation of alcohol from water using the tow fabricated membranes by study the rate of flux. The total permeate flux was increased using PVDF/FMWCNTs membrane compared with pure PVDF membrane due to the hydrophobicity of membrane renders it highly selective to the ethanol than water.

6. REFERENCES

[1] S. Tanaka, T. Iwata, M. Iji, Solvent effects on heterogeneous synthesis of cardanol-bonded cellulose thermoplastics, Polymer (Guildf). 99 (2016) 307–314. https://doi.org/10.1016/J.POLYMER.2016.07.024.

[2] A. Figoli, T. Marino, S. Simone, E. Di Nicolò, X.M. Li, T. He, S. Tornaghi, E. Drioli, Towards non-toxic solvents for membrane preparation: A review, Green Chem. 16 (2014) 4034–4059. https://doi.org/10.1039/C4GC00613E.

[3] F. Russo, C. Ursino, E. Avruscio, G. Desiderio, A. Perrone, S. Santoro, F. Galiano, A. Figoli, Innovative Poly (Vinylidene Fluoride) (PVDF) Electrospun Nanofiber Membrane Preparation Using DMSO as a Low Toxicity Solvent, Membr. 2020, Vol. 10, Page 36. 10 (2020) 36. https://doi.org/10.3390/MEMBRANES10030036.

[4] N. Evenepoel, S. Wen, M. Tilahun Tsehaye, B. Van der Bruggen, Potential of DMSO as greener solvent for PES ultra- and nanofiltration membrane preparation, J. Appl. Polym. Sci. 135 (2018). https://doi.org/10.1002/APP.46494.

[5] D. Matveev, V. Vasilevsky, V. Volkov, T. Plisko, A. Shustikov, A. Volkov, A. Bildyukevich, Fabrication of ultrafiltration membranes from non-toxic solvent dimethylsulfoxide: Benchmarking of commercially available acrylonitrile co-polymers, J. Environ. Chem. Eng. 10 (2022) 107061. https://doi.org/10.1016/J.JECE.2021.107061.

[6] A. Elrasheedy, M. El Kady, M. Bassyouni, T. Yoshitake, A. Elshazly, Enhancement of Antiwetting Properties of Polystyrene Nanofibrous Membrane by Doping with Graphene Nanoplatelets, Mater. Sci. Forum. 1060 (2022) 83–88. https://doi.org/10.4028/P-SUY72P.

[7] N. Khumalo, L. Nthunya, S. Derese, M. Motsa, A. Verliefde, A. Kuvarega, B.B. Mamba, S. Mhlanga, D.S. Dlamini, Water recovery from hydrolysed human urine samples via direct contact membrane distillation using PVDF/PTFE membrane, Sep. Purif. Technol. 211 (2019) 610–617. https://doi.org/10.1016/J.SEPPUR.2018.10.035.

[8] M.O. Midda, A.K. Suresh, Some mechanistic insights into the action of facilitating agents on

Print ISSN 2682-3993
Online ISSN 2682-4000

gas permeation through glassy polymeric membranes, AIChE J. 64 (2018) 186–199. https://doi.org/10.1002/AIC.15873.

[9] H. Espinoza-Gomez, E. Saucedo-Castillo, L.Z. Flores-López, E. Rogel-Hernandez, M. Martínez, F.T. Wakida, Ethanol:water blends separation using ultrafiltration membranes of poly(acrylamide-co-acrylic acid) partial sodium salt and polyacrylamide, Can. J. Chem. Eng. 96 (2018) 763–769. https://doi.org/10.1002/CJCE.23010.

[10] O. Heinz, M. Aghajani, A.R. Greenberg, Y. Ding, Surface-patterning of polymeric membranes: fabrication and performance, Curr. Opin. Chem. Eng. 20 (2018) 1–12. https://doi.org/10.1016/J.COCHE.2018.01.008.

[11] N.F. Himma, N. Prasetya, S. Anisah, I.G. Wenten, Superhydrophobic membrane: Progress in preparation and its separation properties, Rev. Chem. Eng. 35 (2019) 211–238. https://doi.org/10.1515/REVCE-2017-0030/XML.

[12] N. Kosinov, V.G.P. Sripathi, E.J.M. Hensen, Improving separation performance of high-silica zeolite membranes by surface modification with triethoxyfluorosilane, Microporous Mesoporous Mater. 194 (2014) 24–30. https://doi.org/10.1016/J.MICROMESO.2014.03.034.

[13] J.D. Brassard, D.K. Sarkar, J. Perron, Fluorine Based Superhydrophobic Coatings, Appl. Sci. 2012, Vol. 2, Pages 453-464. 2 (2012) 453–464. https://doi.org/10.3390/APP2020453.

[14] C. Picard, A. Larbot, E. Tronel-Peyroz, R. Berjoan, Characterisation of hydrophilic ceramic membranes modified by fluoroalkylsilanes into hydrophobic membranes, Solid State Sci. 6 (2004) 605–612. https://doi.org/10.1016/J.SOLIDSTATESCIENCES.2004.03.017.

[15] A. Marni Sandid, M. Bassyouni, D. Nehari, Y. Elhenawy, Experimental and simulation study of multichannel air gap membrane distillation process with two types of solar collectors, Energy Convers. Manag. 243 (2021) 114431. https://doi.org/10.1016/J.ENCONMAN.2021.114431.

[16] Y. Elhenawy, G.H. Moustafa, S.M.S. Abdel-Hamid, M. Bassyouni, M.M. Elsakka, Experimental investigation of two novel arrangements of air gap membrane distillation module with heat recovery, Energy Reports. 8 (2022) 8563–8573. https://doi.org/10.1016/J.EGYR.2022.06.068.

[17] Y. Elhenawy, G.H. Moustafa, A.M. Attia, A.E. Mansi, T. Majozi, M. Bassyouni, Performance enhancement of a hybrid multi effect evaporation/membrane distillation system driven by solar energy for desalination, J. Environ. Chem. Eng. 10 (2022) 108855. https://doi.org/10.1016/J.JECE.2022.108855.

[18] Y. Elhenawy, K. Fouad, M. Bassyouni, T. Majozi, Design and performance a novel hybrid membrane distillation/humidification–dehumidification system, Energy Convers. Manag. 286 (2023) 117039. https://doi.org/10.1016/J.ENCONMAN.2023.117039.

[19] A.E. Mansi, S.M. El-Marsafy, Y. Elhenawy, M. Bassyouni, Assessing the potential and limitations of membrane-based technologies for the treatment of oilfield produced water, Alexandria Eng. J. 68 (2023) 787–815. https://doi.org/10.1016/J.AEJ.2022.12.013.

[20] G.M. Sessler, Piezoelectricity in polyvinylidenefluoride, J. Acoust. Soc. Am. 70 (1981) 1596–1608. https://doi.org/10.1121/1.387225.

[21] A.J. Lovinger, Ferroelectric Polymers, Science (80-.). 220 (1983) 1115–1121. https://doi.org/10.1126/SCIENCE.220.4602.1115.

[22] P. Martins, A.C. Lopes, S. Lanceros-Mendez, Electroactive phases of poly(vinylidene fluoride): Determination, processing and applications, Prog. Polym. Sci. 39 (2014) 683–706. https://doi.org/10.1016/J.PROGPOLYMSCI.2013.07.006.

[23] Ihsanullah, Carbon nanotube membranes for water purification: Developments, challenges, and prospects for the future, Sep. Purif. Technol. 209 (2019) 307–337. https://doi.org/10.1016/J.SEPPUR.2018.07.043.

[24] F. Fornasiero, Water vapor transport in carbon nanotube membranes and application in breathable and protective fabrics, Curr. Opin. Chem. Eng. 16 (2017) 1–8. https://doi.org/10.1016/J.COCHE.2017.02.001.

[25] M. Majumder, N. Chopra, R. Andrews, B.J. Hinds, Nanoscale hydrodynamics: Enhanced flow in carbon nanotubes, Nature. 438 (2005) 44. https://doi.org/10.1038/43844A.

[26] J.K. Holt, H.G. Park, Y. Wang, M. Stadermann, A.B. Artyukhin, C.P. Grigoropoulos, A. Noy, O. Bakajin, Fast mass transport through sub-2-nanometer carbon nanotubes, Science (80-.). 312 (2006) 1034–1037. https://doi.org/10.1126/SCIENCE.1126298.

[27] S. Li, G. Liao, Z. Liu, Y. Pan, Q. Wu, Y. Weng, X. Zhang, Z. Yang, O.K.C. Tsui, Enhanced water flux in vertically aligned carbon nanotube arrays and polyethersulfone composite membranes, J. Mater. Chem. A. 2 (2014) 12171–12176. https://doi.org/10.1039/C4TA02119C.

Print ISSN 2682-3993
Online ISSN 2682-4000

[28] E. Fontananova, V. Grosso, S.A. Aljlil, M.A. Bahattab, D. Vuono, F.P. Nicoletta, E. Curcio, E. Drioli, G. Di Profio, Effect of functional groups on the properties of multiwalled carbon nanotubes/polyvinylidenefluoride composite membranes, J. Memb. Sci. 541 (2009) 198–204. https://doi.org/10.1016/J.MEMSCI.2017.07.002.
[29] D. Yang, C. Cheng, M. Bao, L. Chen, Y. Bao, C. Xue, The pervaporative membrane with vertically aligned carbon nanotube nanochannel for enhancing butanol recovery, J. Memb. Sci. 577 (2019) 51–59. https://doi.org/10.1016/J.MEMSCI.2019.01.032.
[30] P.K. Burnwal, P. Pal, M.O. Midda, S.P. Chaurasia, Synthesis of Hybrid PVDF–PTFE Membrane Using Nonhazardous Solvent for Ethanol–Water Separation through Membrane Distillation, J. Hazardous, Toxic, Radioact. Waste. 26 (2022). https://doi.org/10.1061/(ASCE)HZ.2153-5515.0000710.
[31] R. Dallaev, T. Pisarenko, D. Sobola, F. Orudzhev, S. Ramazanov, T. Trčka, Brief Review of PVDF Properties and Applications Potential, Polym. 2022, Vol. 14, Page 4793. 14 (2022) 4793. https://doi.org/10.3390/POLYM14224793.
[32] T.L.S. Silva, S. Morales-Torres, J.L. Figueiredo, A.M.T. Silva, Multi-walled carbon nanotube/PVDF blended membranes with sponge- and finger-like pores for direct contact membrane distillation, Desalination. 357 (2015) 233–245. https://doi.org/10.1016/J.DESAL.2014.11.025.
[33] J.M. Park, G.Y. Gu, Z.J. Wang, D.J. Kwon, P.S. Shin, J.Y. Choi, K. Lawrence DeVries, Mechanical and electrical properties of electrospun CNT/PVDF nanofiber for micro-actuator applications, Adv. Compos. Mater. 25 (2016) 305–316. https://doi.org/10.1080/09243046.2015.1082714.
[34] J. Ma, Y. Zhao, Z. Xu, C. Min, B. Zhou, Y. Li, B. Li, J. Niu, Role of oxygen-containing groups on MWCNTs in enhanced separation and permeability performance for PVDF hybrid ultrafiltration membranes, Desalination. 320 (2013) 1–9. https://doi.org/10.1016/J.DESAL.2013.04.012.
[35] M. Mofakhami Mehrabadi, A. Aghaei, M. Sahba Yaghmaee, M. Karimnezhad, M. Kamari, The effect of functional carbon nanotubes on the permeability of ultrafiltration nanocomposite PVDF membranes, Asia-Pacific J. Chem. Eng. 13 (2018). https://doi.org/10.1002/APJ.2180.
[36] M.A.E.R. Abu-Zeid, Y. Zhang, H. Dong, L. Zhang, H.L. Chen, L. Hou, A comprehensive review of vacuum membrane distillation technique, Desalination. 356 (2015) 1–14. https://doi.org/10.1016/J.DESAL.2014.10.033.
[37] R.M. Zarraa, S.A. Nosier, A.A. Zatout, M.H.A. Abdel-aziz, M.S. Al-Geundi, Efficient Ethanol Separation from Water Using Vacuum Membrane Distillation, Egypt. J. Chem. 0 (2023) 0–0. https://doi.org/10.21608/EJCHEM.2023.227328.8370.
[38] M. Niamat, S. Sarfraz, E. Shehab, S.O. Ismail, Q.S. Khalid, Experimental Characterization of Electrical Discharge Machining of Aluminum 6061 T6 Alloy using Different Dielectrics, Arab. J. Sci. Eng. 44 (2019) 8043–8052. https://doi.org/10.1007/S13369-019-03987-4.
[39] M.A. Mohamed, J. Jaafar, A.F. Ismail, M.H.D. Othman, M.A. Rahman, Fourier Transform Infrared (FTIR) Spectroscopy, Membr. Charact. (2017) 3–29. https://doi.org/10.1016/B978-0-444-63776-5.00001-2.
[40] T. Huhtamäki, X. Tian, J.T. Korhonen, R.H.A. Ras, Surface-wetting characterization using contact-angle measurements, Nat. Protoc. 13 (2018) 1521–1538. https://doi.org/10.1038/S41596-018-0003-Z.
[41] X. Wang, L. Zhang, D. Sun, Q. An, H. Chen, Formation mechanism and crystallization of poly(vinylidene fluoride) membrane via immersion precipitation method, Desalination. 236 (2009) 170–178. https://doi.org/10.1016/J.DESAL.2007.10.064.
[42] A. Elrasheedy, M. Rabie, A. El-Shazly, M. Bassyouni, S.M.S. Abdel-Hamid, M.F. El Kady, Numerical Investigation of Fabricated MWCNTs/Polystyrene Nanofibrous Membrane for DCMD, Polym. 2021, Vol. 13, Page 160. 13 (2021) 160. https://doi.org/10.3390/POLYM13010160.
[43] R. Kotsilkova, I. Borovanska, P. Todorov, E. Ivanov, D. Menseidov, S. Chakraborty, C. Bhattacharjee, Tensile and Surface Mechanical Properties of Polyethersulphone (PES) and Polyvinylidene Fluoride (PVDF) Membranes, J. Theor. Appl. Mech. 48 (2018) 85–99. https://doi.org/10.2478/JTAM-2018-0018.
[44] I. Ali, O.A. Bamaga, L. Gzara, M. Bassyouni, M.H. Abdel-Aziz, M.F. Soliman, E. Drioli, M. Albeirutty, Assessment of Blend PVDF Membranes, and the Effect of Polymer Concentration and Blend Composition, Membr. 2018, Vol. 8, Page 13. 8 (2018) 13. https://doi.org/10.3390/MEMBRANES8010013.

Print ISSN 2682-3993
Online ISSN 2682-4000

[45] B. Hudaib, R. Abu-Zurayk, H. Waleed, A.A. Ibrahim, Fabrication of a Novel (PVDF/MWCNT/Polypyrrole) Antifouling High Flux Ultrafiltration Membrane for Crude Oil Wastewater Treatment, Membranes (Basel). 12 (2022). https://doi.org/10.3390/MEMBRANES12080751.

[46] J. hui Yang, Y. jun Xiao, C. jin Yang, S. tai Li, X. dong Qi, Y. Wang, Multifunctional poly(vinylidene fluoride) nanocomposites via incorporation of ionic liquid coated carbon nanotubes, Eur. Polym. J. 98 (2018) 375–383. https://doi.org/10.1016/J.EURPOLYMJ.2017.11.037.

[47] S. Mishra, K.T. Kumaran, R. Sivakumaran, S.P. Pandian, S. Kundu, Synthesis of PVDF/CNT and their functionalized composites for studying their electrical properties to analyze their applicability in actuation & sensing, Colloids Surfaces A Physicochem. Eng. Asp. 509 (2016) 684–696. https://doi.org/10.1016/J.COLSURFA.2016.09.007.

[48] W. Bin Zhang, Z.X. Zhang, J.H. Yang, T. Huang, N. Zhang, X.T. Zheng, Y. Wang, Z.W. Zhou, Largely enhanced thermal conductivity of poly(vinylidene fluoride)/carbon nanotube composites achieved by adding graphene oxide, Carbon N. Y. 90 (2015) 242–254. https://doi.org/10.1016/J.CARBON.2015.04.040.

[49] R. Zhou, D. Rana, T. Matsuura, C.Q. Lan, Effects of multi-walled carbon nanotubes (MWCNTs) and integrated MWCNTs/SiO2 nano-additives on PVDF polymeric membranes for vacuum membrane distillation, Sep. Purif. Technol. 217 (2019) 154–163. https://doi.org/10.1016/J.SEPPUR.2019.02.013.